National Conference with International Participation
ENGINEERING MECHANICS 2001
Svratka, Czech Republic, May 14 – 17, 2001

NUMERICAL SIMULATION OF THE CARDIOVASCULAR HEMODYNAMICS DURING HEMORRHAGING

Světlana Převorovská*, František Maršík†

Summary: *The numerical model of the cardiovascular system of pulsating type including the model of the electrochemical and mechanical heart muscle activity and the short-term baroreflex control has been implemented to achieve more accurate diagnostics of a patient hemodynamic profile. This model enables the simulation of the hemodynamic reaction activity as consequence of the baroreflex response to various perturbations in the circulatory system. The hemodynamic behaviour of the cardiovascular system in case of the circulatory failure caused by hemorrhagic shock is demonstrated.*

Key words: *cardiovascular hemodynamics, numerical simulation, baroreflex control, hemorrhagic shock*

1 Introduction

The baroreflex short-term control of the cardiovascular system is a regulatory feedback loop which preserves maintaining the blood pressure at adequate level to perfuse body tissues and thus guarantees the oxygen delivery to all beds. The control loop involves the autonomic nervous system (ANS) with parasympathetic and sympathetic paths, the chemoreceptors, and the baroreceptors (i.e. specialized tissue cells behaving as stretch receptors located in the walls of the heart and blood vessels; the baroreceptors located in the wall of the aortic arch and carotid arteries monitor the arterial circulation). The changes of the blood pressure are perceived by the baroreceptors which send signals to the ANS regulating the sympathetic and parasympathetic (vagal) system output. The sympathetic and vagal activities continually interact, a decrease of vagal activity accompanies an increase of sympathetic activity and vice versa. Consequently the reaction on the blood pressure drop results in an increase of the sympathetic activity and a decrease in the vagal activity. The sympathetic tone rises of the heart rate (the chronotropic effect), increases the myocardial contractility (the inotropic effect) and causes the vasoconstriction of the blood vessels (i.e. increases theirs resistance). The vagal tone slows the heart rate and causes the blood vessels vasodilatation (i.e. decreases their resistance). The response on the blood pressure increase has the contrary effect, the vagal tone rises and the sympathetic tone decreases. The baroreflex control affects the heart rate and the vascular compliance, resistance, myocardial contractility as well. The baroreflex reflects various perturbations in the cardiovascular system and causes thus the hemodynamic changes trying to restore the system to its initial physiological state.

*Ing. Světlana Převorovská, Ústav termomechaniky AV ČR, Dolejškova 5, 182 00 Praha 8; tel. +420 2 6605 3342, e–mail: svetlana@it.cas.cz

†Prof. František Maršík, DrSc., Ústav termomechaniky AV ČR, Dolejškova 5, 182 00 Praha 8; tel. +420 2 6605 3322, e–mail:marsik@it.cas.cz

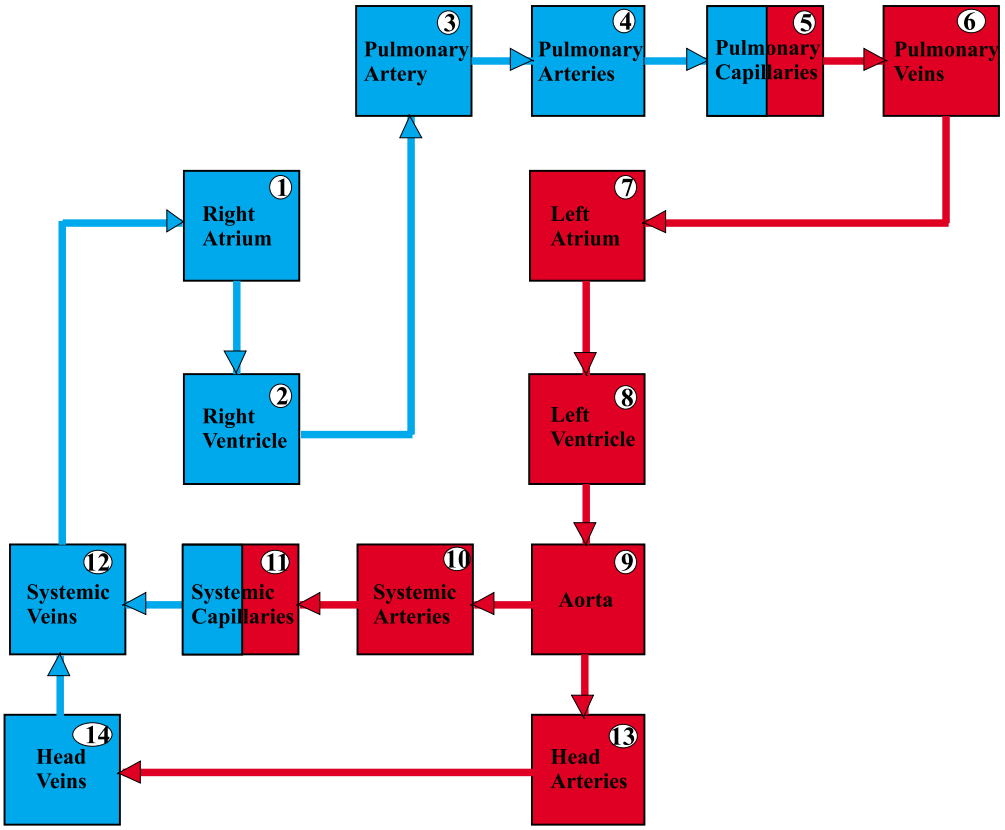

Figure 1: *The scheme of the cardiovascular system (CVS)*

2 Mathematical model of the human cardiovascular system

For the modeling purposes the real cardiovascular system has been compartmentalized, the simplified scheme see on the Fig. 1. The circulatory system is modelled by four compartments of a pulsating heart: the right and left atria (they are numbered in the CVS scheme 1, 7), the right and left ventricles (2, 8) and by ten vascular segments of the pulmonary and systemic circuits connected with the heart in series. The pulmonary circuit consists of pulmonary artery (3), arteries and arterioles (4), capillaries (5), veins (6). The systemic circulation contains the aorta (9), arteries, arterioles (10), capillaries (11) and veins (12), head arteries (13) and head veins (14).

The suggested model provides the one-dimensional flow of the incompressible blood through the network of elastic blood vessels. The heart segments are considered as anisotropic and viscoelastic incompressible material. The behaviour of the cardiovascular system is described by its hemodynamical variables, i.e. the blood pressure, volume and by the cardiovascular parameters such as the compliance and resistance of corresponding compartments. The blood inertia and the physico-chemical variables such as the cardiac action potential, the calcium concentration are included to model the performance of cardiovascular system more precisely.

2.1 Chemo-mechanical performance of heart

The pressure pulsation in the heart compartments working as a pressure-volume pumps are generated by calcium kinetics which plays central role in the generation of the action potentials of the cardiac myocytes. For the description of the cardiac action membrane potentials and the concentration changes of the calcium ions transported through the cardiac myocyte membrane the Beeler-Reuter equations [1] are used. The used equations are applied on heart segments

numbered in the scheme on the Fig. (1) $i = 1, 2, 7, 8$ The atrial and ventricular action potentials $V_{m_i}\,[mV]$ are determined by four major ionic currents I_{Na_i} (i.e. the fast inward sodium current), I_{s_i} (the slow inward calcium current), I_{K_i} (the time-independent potassium current), I_{x_i} (the time-dependent outward potassium current)

$$\frac{dV_{m_i}(t)}{dt} = -\frac{1}{C_m}\left(I_{Na_i}(t) + I_{s_i}(t) + I_{K_i}(t) + I_{x_i}(t) - I_{st_i}(t)\right)\,, \tag{1}$$

$C_m\,[\mu F/cm^2]$ is the myocardial tissue's capacitance, $I_{st_i}\,[\mu A/cm^2]$ is the stimulating current. The ionic currents in the i-th segments are given

$$I_{Na_i}(t) = \left(g_{Na_i} m_i^3(t) h_i(t) j_i(t) + g_{NaC_i}\right)\left(V_{m_i}(t) - E_{Na}\right)\,, \quad E_{Na} = \frac{RT}{ZF}\ln\frac{c_{Na_o}}{c_{Na_{in}}}\,, \tag{2}$$

$$I_{s_i}(t) = g_{s_i} d_i(t) f_i(t)\left(V_{m_i}(t) - E_{s_i}(t)\right)\,, \quad E_{s_i}(t) = -82,3 - 13,0287\ln c_{Ca_i}(t)\,, \tag{3}$$

$$I_{K_i}(t) = 0,35 g_{K_i}\left[4\frac{e^{0,04\left(V_{m_i}(t)+85\right)} - 1}{e^{0,08\left(V_{m_i}(t)+53\right)} + e^{0,04\left(V_{m_i}(t)+53\right)}} + 0,2\frac{V_{m_i}(t) + 23}{1 - e^{-0,04\left(V_{m_i}(t)+27\right)}}\right]\,, \tag{4}$$

$$I_{x_i}(t) = 0,8 g_{x_i} x_i(t)\frac{e^{0,04\left(V_{m_i}(t)+77\right)} - 1}{e^{0,04\left(V_{m_i}(t)+35\right)}}\,. \tag{5}$$

The symbols in the equations (2-5) for the calculation of the ionic currents mean

$c_{Na_{ex}}\,, c_{Na_{in}}$	$[mM]$	extracellular, intracellular sodium ion concentration,
c_{Ca_i}	$[mM]$	intracellular calcium ion concentration,
$F = 96,485$	$[C/M]$	Faraday constant,
$g_{Na_i}\,, g_{NaC_i}$	$[mS/cm^2]$	sodium channels conductance,
g_{s_i}	$[mS/cm^2]$	calcium channels conductance,
$g_{K_i}\,, g_{x_i}$	$[mS/cm^2]$	potassium channels conductance,
E_{Na}, E_s	$[mV]$	Nernst equilibrium potential of $Na^+\,, Ca^{2+}$ ions,
$m_i, h_i, j_i, d_i, f_i, x_i = y$	[1]	gating variables determining channel, opening and closing,
$R = 8,3143$	$[J/M\,K]$	gas constant,
T	$[K]$	temperature ($T \doteq 310\,K$),
Z	[1]	ionic charge number, for Na^+ $Z = 1$.

The gating variables are defined by the differential equation $\frac{dy_i(t)}{dt} = (y_{\infty_i}(t) - y_i(t))/\tau_{y_i}(t)$ where $y_{\infty_i}(t) = \alpha_{y_i}(t)/(\alpha_{y_i}(t) + \beta_{y_i}(t))$, denotes the steady state fraction of open channels, $\tau_{y_i}(t) = 1/(\alpha_{y_i}(t) + \beta_{y_i}(t))$ is the relaxation time, $\alpha_{y_i}\,, \beta_{y_i}$ are the rate constants depending on the transmembrane potential V_m, see [1].

The calcium ion intracellular concentration $c_{Ca_i}\,[mM]$ is calculated by the following differential equation

$$\frac{dc_{Ca_i(t)}}{dt} = -10^{-7} I_{s_i} + 0,07\left(10^{-7} - c_{Ca_i(t)}\right)\,. \tag{6}$$

The concentration of the Ca^{2+} ions regulates the force of myocardial contraction i.e. the generated pressure by the contracting heart. The pressures in the heart atria and ventricles are described by the equation derived from the general energy and entropy balance (see [2])

$$p_i(t) = \frac{2h_i E_i}{r_i}\left(\frac{V_i(t)}{V_{oi}} - 1\right) + \frac{2h_i k_{chem,\,i}}{r_i} c_{Ca_i}(t)\,, \quad i = 1, 2, 7, 8\,, \tag{7}$$

in which parameters in i-th segment are

c_{Ca_i}	$[mM]$	calcium concentration,
E_i	$[J/m^3]$	Young's elasticity module,
h_i	$[m]$	thickness of the atrial and ventricular walls,
$k_{chemi,i}$	$[J/m^3M]$	parameter of the chemical energy release,
p_i	$[Pa = \frac{J}{m^3}]$	atrial or ventricular pressure,
r_i	$[m]$	radius of the atria or ventricles,
V_i	$[m^3]$	atrial or ventricular volume,
V_{oi}	$[m^3]$	initial atrial or ventricular volume.

The first term on the right hand side of Eq. (7) describes the elasticity of the heart and the second term expresses the transformation of chemical energy into mechanical one.

2.2 Hemodynamic performance of the cardiovascular system

The pressure changes in the pulmonary artery and aorta are described

$$p_i(t) = \frac{1}{C_i}\left(V_i(t) - V_{res_i}\right) + \eta_i \frac{dV_i(t)}{dt}\,, \quad i = 3, 9 \tag{8}$$

and in other segments of the pulmonary and systemic circuit

$$p_i(t) = \frac{1}{C_i}\left(V_i(t) - V_{res_i}\right)\,, \quad i = 4, 5, 6, 10, 11, 12, 13, 14\,, \tag{9}$$

where $C_i\,[m^3/Pa]$ denotes the compliance, $V_{res_i}\,[m^3]$ is the residual volume of the i-th segment, $\eta_i\,[Pa\,s/m^3]$ represents the wall viscosity.

The blood flow $F_{ij}\,[m^3/s]$ between the i-th and j-th segments is determined by the balance of the momentum in the following forms:

$i = 2, 8$, $j = 3, 9$ (flow between the ventricles and output arteries, i.e. the pulmonary artery and the aorta)

$$\frac{dF_{ij}(t)}{dt} = \frac{1}{L_i}\left[p_i(t) - p_j(t) - R_{ij}F_{ij}(t) - \xi^2\frac{\rho F_{ij}^2(t)}{2A_i^2(t)}\right]\,, \quad A_i(t) = \frac{60\,F_{ij}(t)}{t_{VS}HR\sqrt{2(p_i(t) - p_j(t))/\rho}}\,, \tag{10}$$

where $R_{ij}\,[Pa\,s/m^3]$ is the hydrodynamical resistance, $L_i\,[Pa\,s^2/m^3]$ characterizes the blood inertia, $\xi\,[1]$ is the blood inertia coefficient, $A_i\,[m^2]$ is the flow area, $HR\,[beats/min]$ is the heart rate, $t_{VS}\,[s]$ is the time duration of the ventricular systole, $\rho = 1,062.10^3\,[kg/m^3]$ is the blood density,

$i = 3, 9, 9$, $j = 4, 10, 13$ (flow between the arterial segments)

$$\frac{dF_{ij}(t)}{dt} = \frac{1}{L_i}\left[p_i(t) - p_j(t) - R_{ij}F_{ij}(t)\right]\,, \tag{11}$$

$i = 1, 7, 6, 12, 13$, $j = 2, 8, 7, 1, 14$ (flow between the atria and ventricles, the pulmonary and systemic veins and atria, between the head artery and head veins)

$$F_{ij}(t) = \frac{p_i(t) - p_j(t)}{R_{ij}}\,, \tag{12}$$

$i = 4, 10, 11, 14, 5$, $j = 5, 11, 12, 12, 6$ (flow between arterial segments, capillaries and veins)

$$F_{ij}(t) = \frac{(p_i(t) - p_j(t))\, V_i^2(t)}{R_{ij} V_{res_i}^2} \,. \tag{13}$$

The volume changes in all considered segments of the cardiovascular system are determined by the balance of mass

$$\frac{dV_i(t)}{dt} = F_{ij}(t) - F_{jk}(t)\,, \quad i,j,k = 1,2,...,14\,, \tag{14}$$

F_{ij}, F_{jk} are the blood flow entering from the i-th to j-th segment, resp. the blood flow getting out j-th to k-th segment.

2.3 Baroreflex control

The modeling equations of baroreflex control adopted from [3] describe

- the baroreceptor activity [1] $\nu_a\,[1]$ which is affected both by the blood pressure and the rate of pressure change

$$\nu_a = k_1\,(P - P_o) + k_2 \frac{dP}{dt}\,, \tag{15}$$

where $P\,[mmHg]$ is mean value of blood pressure, $P_o\,[mmHg]$ is the threshold pressure below which the firing of the baroreceptor does not occur and $k_1\,[1/mmHg]$, $k_2\,[s/mmHg]$ are constants,

- sympathetic activity $\nu_s\,[1]$

$$\nu_s = \nu_s^o - k_s \nu_a + k_s^r \left|\sin\left(\pi f_r t + \Delta\phi_s^r\right)\right|\,, \tag{16}$$

$f_r\,[1/s]$ is the respiratory frequency, $\nu_s^o\,[1], k_s\,[1], k_s^r\,[1], \Delta\phi_s^r\,[1]$ are constants,

- parasympathetic activity $\nu_p\,[1]$

$$\nu_p = \nu_p^o - k_p \nu_a + k_p^r \left|\sin\left(\pi f_r t + \Delta\phi_p^r\right)\right|\,, \tag{17}$$

$\nu_p^o\,[1], k_p\,[1], k_p^r\,[1], \Delta\phi_p^r\,[1]$ are constants.

The baroreflex control of the heart rate $HR\,[beat/min]$ is the result of balance between the sympathetic and vagal activity as follows

$$HR = HR^o \left[1 + \frac{\nu_s}{HR^o\,(c_1 + c_2\nu_s)}\right] \left[1 - \frac{\nu_p}{HR^o\,(c_3 + c_4\nu_p)}\right]\,, \tag{18}$$

$HR^o\,[beat/min]$ is the resting heart rate, c_1, c_2, c_3, c_4 $[min/beat]$ are constants. Consequently, if the heart rate changes, the cardiac cycle duration is altered. The following dependencies of the atrial systole ($t_{AS}\,[s]$) or ventricular systole ($t_{VS}\,[s]$) duration on the heart rate stated by the regression method from the clinical data are used

$$t_{AS} = 0,4056 - 0,0083(HR) + 8.10^5(HR)^2 - 3,6631.10^{-7}(HR)^3 + 6,3447.10^{-10}(HR)^4\,, \tag{19}$$

$$t_{VS} = 0,404 - 0,016(HR)\,. \tag{20}$$

[1] above mentioned authors consider one baroreceptor, in the described model here the aortic and carotid baroreceptors are used, their activities are summed up: $\nu_a = 0,3\nu_{a_{Ao}} + 0,7\nu_{a_{HA}}$

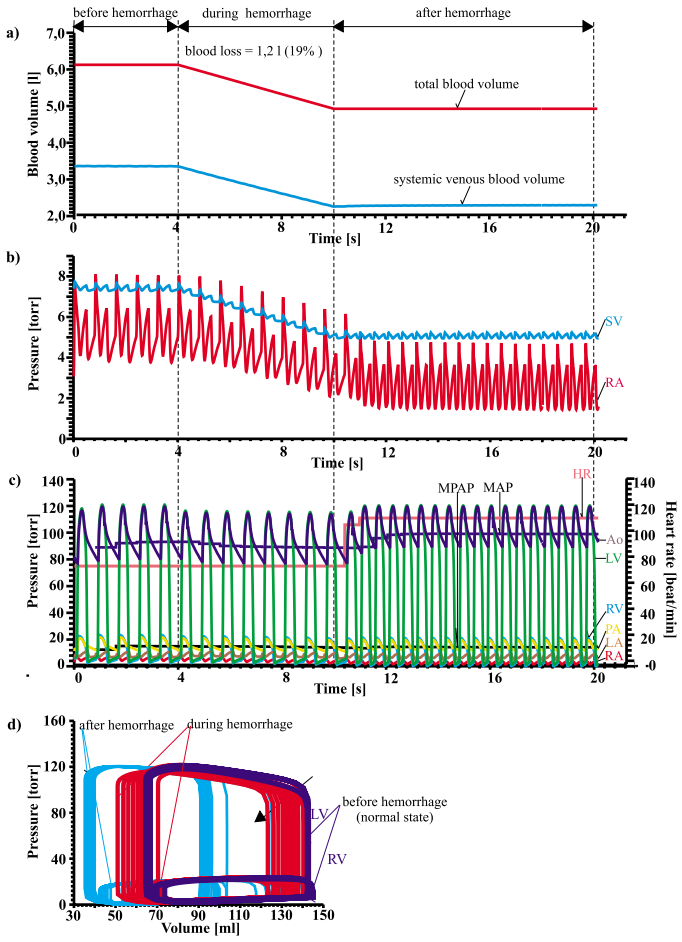

Figure 2: *Simulation of the II. class hemorrhagic shock*

2.4 Results of the numerical simulation of the blood loss

The hemodynamic changes in the cardiovascular system caused by the baroreflex response on hemorrhage depend on the amount of the blood loss. Four classes of the hemorrhagic shock are distinguished (see e.g. [4], [5]). The simulated results summarized in the Table 1 and depicted on the Fig. 2 demonstrate the hemodynamic responses corresponding to the shock of II. class, that means the blood volume reduction is in the range of $15-30\%$, i.e. $750-1500\,ml$ of the total blood volume in the cardiovascular system. The following hemodynamic changes accompanying this shock state (during the simulated venous hemorrhage the decrease of the total blood volume was $1,2\,l$, i.e. 19%, see Fig. 2a) are decreased

- systemic venous (SV) and right atrial (RA) pressures (documented on the Fig. 2b),

- arterial (Ao, PA) and ventricular pressures (LV, RV) (Fig. 2c),

- left and right ventricular systolic and diastolic volume and their stroke volume (Fig. 2d),

- cardiac output and venous return (Table 1)

- myocardial oxygen consumption (Table 1)

The blood loss triggers a compensatory baroreflex control evoking vasoconstriction (especially of the arterioles), i.e. an increase of the systemic and pulmonary vascular resistances (see results in the Table 1) and tachycardia (i.e. an increase of the heart rate, see results in the Table 1 and

Table 1: Simulated hemodynamic profile under the normal state, during and after hemorrhage

hemodynamic parameters		**normal state**	**during hemorrhage**	**after hemorrhage**
Heart rate	$[beat/min]$	75	106	111
Cardiac output	$[l/min]$	5,6	5,4	6,2
Venous return	$[l/min]$	5,6	4,0	6,3
Left ventricle end diastolic volume	$[ml]$	141,0	123,4	91,0
Left ventricle end systolic volume	$[ml]$	65,3	50,8	35,2
Stroke volume	$[ml]$	75,6	72,6	55,8
Left ventricular stroke work	$[g\,m]$	87,4	80,2	70,3
Right ventricular stroke work	$[g\,m]$	10,5	9,0	8,8
Mean arterial pressure	$[torr]$	93,2	88,6	99
Mean right atrial pressure	$[torr]$	5,2	3,5	2,5
Mean filling pressure	$[torr]$	7,4	5,1	5,0
Mean pulmonary artery pressure	$[torr]$	15,0	13,8	14,2
Systemic vascular resistance	$[dyn\,s/cm^5]$	1240,7	1250,6	1245,9
Pulmonary vascular resistance	$[dyn\,s/cm^5]$	94,9	107,2	101,6
Myocardial oxygen consumption	$[J/beat]$	3,26	2,84	2,34
Myocardial efficiency	$[\%]$	28,8	30,3	32,0

Fig. 2c)). After this compensation the systolic pressures in the aorta, pulmonary artery and in both ventricles restore to the initial level , the diastolic aortic and pulmonary artery pressures increase (i.e. the pulse pressure decreases and thus the values of the mean aortic and pulmonary artery pressures MAP, $MPAP$ increase), (Fig. 2c). The cardiac output and venous return are elevated in consequence of the tachycardia. The vasoconstriction of blood vessels diminishes, i.e. their resistance decreases.

If the blood loss is less than 15% of the blood volume the arterial blood pressure does not record measurable changes. The venous pressure is a better indicator of the hemorrhage severity.

Conclusion

Mathematical models of the cardiovascular system are useful tools to deeper understanding of complex processes, occuring in the heart and blood vessels under the normal or pathophysiological states. The proposed fourteen segment hemodynamic model enables the simulation of the electrochemical and mechanical heart actions and the hemodynamic response of the whole cardiovascular system under various perturbations. As an example of the baroreflex response to cardiovascular system perturbation the suggested model has been used to demonstrate the hemodynamic changes caused by the circulatory failure during the sudden volume decrease. The resulting hemorrhagic shock represents the insufficient oxygen and other nutrients delivery, followed by the metabolic demands of the body tissues which can not be satisfied. The pressure waves, volume changes in all compartments and flows between them during cardiac cycles and complex hemodynamic profile evaluated from these variables under various conditions can be used for diagnostics of a patients. The simulation results are compatible with the published clinical data and are further simultaneously tested in clinical practice.

Acknowledgement

This research is supported by the Pilot project of IT CAS No.50258.

References

[1] G.W. Beeler, H. Reuter. Reconstruction of the action potential of ventricular myocardial fibres. *J.Physiol. (Lond.)*, **268** , 177–210, (1977).

[2] S. Převorovská, F. Maršík. The influence of the membrane transport on the heart mechanical activity. *Engineering mechanics'99, Svratka, May 17-20*, 575-580, (1999)

[3] H. Seidel, A. Herzel. Modeling heart rate variability due to respiration and baroreflex. In E. Mosekilde and O.G. Mouritsen, ed. *Modeling the Dynamics of Biological Systems*, pages 205-229, Springer-Verlag, Berlin, (1995).

[4] S. Neumann. Modeling acute hemorrhage in the human cardiovascular system. A dissertation bioengineering, University of Pensylvania, (1996).

[5] I. H. Wilson, O.J.F. Baskett. The diagnosis and treatment of haemorrhagic shock. Practical Procedures, Issue 1, Article 4, (1992).